

Tip-to-base conduit widening remains consistent across cambial age and climates in *Fagus sylvatica* L.

Angelo Rita^{1,*} , Osvaldo Pericolo^{2,3}, Jan Tumajer⁴, Francesco Ripullone² , Tiziana Gentilesca², Antonio Saracino¹ , Marco Borghetti²

¹Dipartimento di Agraria, Università degli Studi di Napoli Federico II, Piazza Carlo di Borbone 1, I-80055 Portici (Napoli), Italy

²Scuola di Scienze Agrarie, Forestali, Alimentari ed Ambientali, Università degli Studi della Basilicata, viale dell'Ateneo Lucano 10, I-85100 Potenza, Italy

³Dipartimento di Scienze della Terra e dell'Ambiente, Università di Pavia, via S. Epifanio 14, I-27100 Pavia, Italy

⁴Department of Physical Geography and Geoecology, Charles University, Faculty of Science, Albertov 6, CZ-12843 Prague, Czech Republic

*Corresponding author: Dipartimento di Agraria, Università degli Studi di Napoli Federico II, Piazza Carlo di Borbone 1, I-80055 Portici (Napoli), Italy, Email: angelo.rita@unina.it

Handling Editor: Frederick Meinzer

Water transport, mechanical support and storage are the vital functions provided by the xylem. These functions are carried out by different cells, exhibiting significant anatomical variation not only within species but also within individual trees. In this study, we used a comprehensive dataset to investigate the consistency of predicted hydraulic vessel diameter widening values in relation to the distance from the tree apex, represented by the relationship $D_h \propto L^\beta$ (where D_h is the hydraulic vessel diameter, L the distance from the stem apex and β the scaling exponent). Our analysis involved 10 *Fagus sylvatica* L. trees sampled at two distinct sites in the Italian Apennines. Our results strongly emphasize that vessel diameter follows a predictable pattern with the distance from the stem apex and $\beta \sim 0.20$ remains consistent across cambial age and climates. This finding supports the hypothesis that trees do not alter their axial configuration represented by scaling of vessel diameter to compensate for hydraulic limitations imposed by tree height during growth. The study further indicates that within-tree variability significantly contributes to the overall variance of the vessel diameter-stem length exponent. Understanding the factors that contribute to the intraindividual variability in the widening exponent is essential, particularly in relation to interspecific responses and adaptations to drought stress.

Key words: allometry, architecture, diffuse-porous, hydraulic, quantitative wood anatomy, vessels, xylem traits..

Introduction

Water uptake and transport in vascular plants play a pivotal role in several developmental processes, including transpiration, photosynthesis and nutrient uptake. As long-living organisms, trees undergo structural and functional changes during ontogeny, which require steady adjustments in xylem hydraulic architecture in response to ever-increasing distances over which water must be transported (Meinzer et al. 2011). Regardless of their differences in growth rate and plant habit, trees encounter a common challenge as they grow taller in order to maintain water transport efficiency and conductance per unit leaf area. This challenge arises from flow resistance, proportional to the total path length, as trees increase in height. To maintain a constant conductance per unit leaf area and supply a branching canopy, vessels must widen proportionally from the tip to the base of the stem as individual plants grow taller. However, while a set of large xylem conduits can have lower overall carbon costs than smaller conduits with the same hydraulic conductance, this efficiency comes with the potential cost of increased vulnerability to embolism (Hacke et al. 2006, 2023; Jacobsen and Pratt 2023, but see Hajek et al. 2016). Consequently, to ensure water transport through plants, xylem conductance, embolism vulnerability and the construction costs of the conducting system must be carefully balanced as trees grow taller. Because of the importance of this equilibrium in plant hydraulic evolution and

forest responses to climate change, optimality models have been developed over the past few decades to predict how and why plants vary vessels diameters throughout their bodies. Several conflicting theories have been proposed to describe the coordination between tree size and vascular architecture. Some models implicitly assume constant vessel diameter (e.g. Shinozaki et al. 1964a, b), while others predict that they widen from tip to base (e.g. West et al. 1999; Savage et al. 2010). Among them, the theoretical West, Brown and Enquist (WBE, West et al. 1997, 1999) model posits that the fractal-like geometry found in many biological systems is the fundamental basis for the allometric scaling observed in the vascular plant transport system. Empirical measurements strongly indicate that vessel lumen areas will narrow axially from tree base to stem apex and branches with the power function as the distance from the tree apex increases, as observed in a wide range of species, across individuals of different heights as well as across different taxa (Anfodillo et al. 2006; Prendin et al. 2018; Koçillari et al. 2021; Petit et al. 2023 among the others). This consistent axial scaling is a common trait across a wide range of tree species, suggesting that natural selection primarily shapes the distribution of xylem vessels diameter along the axis through uniform biophysical principles governing plant functional integrity, rather than through niche differentiation and divergent ecological strategies (Anfodillo et al. 2013; Olson et al. 2014; Williams et al. 2019; Zhong et al. 2019).

Received: December 7, 2023. Revised: June 17, 2024. Accepted: July 1, 2024

© The Author(s) 2024. Published by Oxford University Press.

This is an Open Access article distributed under the terms of the Creative Commons Attribution Non-Commercial License

(<https://creativecommons.org/licenses/by-nc/4.0/>), which permits non-commercial re-use, distribution, and reproduction in any medium, provided the original work is properly cited. For commercial re-use, please contact journals.permissions@oup.com

Along the xylem pathway, the vessels' widening pattern is well approximated by the power function $y = \alpha \cdot L^\beta$, where y represents the vessel hydraulic diameter, α is the allometric constant, L is the distance from stem apex and β is the tip-to-base vessel widening exponent, which describes the rate of basipetal widening. A zero-value β indicates vessels of uniform diameter as the pipe model implicitly assumes (Shinozaki et al. 1964a, b), whereas larger β values indicate greater rates of axial widening. According to the theoretical WBE model (West et al. 1999), a vascular design that fully compensates for the progressive increase in hydraulic resistance with tree height should have an ideal vessel diameter widening exponent $\beta = 0.25$ (for the idealized plant of the WBE model) and translates into $\beta \sim 0.2$ when the scaling is between vessel diameter and distance from the stem apex (Becker et al. 2000; Anfodillo et al. 2006; Petit and Anfodillo 2009). However, from several studies it has emerged that the rate of vessel widening (β) varies across tree species, habit and growth environment, typically ranging from ≈ 0.13 to ≈ 0.34 (Petit et al. 2010, 2011; Pfautsch et al. 2018; Williams et al. 2019), for reasons that are currently not entirely clear. Even well-established models contain assumptions that require further testing and await the incorporation of novel empirical observations. In fact, since the publication of the WBE model, several criticisms have been highlighted that question its basic framework, assumptions and generality and reveal empirical patterns that contradict parts of the WBE model. Savage et al. (2010) tried to improve the theory's representation of vascular architecture, highlighting how hydraulic safety and efficiency may have shaped the evolution of vascular networks (but see Sopp and Valbuena 2023). That is, the packing rule contradicts the premise of the WBE model that vessel frequency remains constant as vessel radii taper. Other studies over the past few years have reported new empirical observations that are waiting to be incorporated into hydraulic models. For instance, taller plants have broader vessels at the base because of tip-to-base vessel widening, as well as wider terminal vessels (e.g. Olson et al. 2018) thought to be the result of selection maintaining a constant leaf-specific sapwood conductance with height increase. Lechthaler et al. (2019a, 2020) found for *Acer pseudoplatanus* L. that vessels in leaf veins enlarge from their termination toward the petiole base, twice to how they behave in stems. Further, in profiles of diameter from tip to base, vessels close to the stem base are frequently found to be narrower than expected (Petit and Anfodillo 2009; Olson et al. 2018; Pfautsch et al. 2018, but see Koçillari et al. 2021).

From the above it has emerged that there are still many outstanding issues regarding the variability of xylem anatomical traits as an individual tree grows taller, which currently limits a full understanding of vessel scaling patterns along the stem flow path (see Rosell et al. 2017 and Olson et al. 2021 for an overview). Among them, the vessel diameter is expected to widen with distance from the stem tip according to a power law ($D_b \propto L^\beta$); however, not all observations confirmed a precise value or a strict power-like pattern of β , the vessel widening exponent. Furthermore, although tip-to-base vessel widening has been demonstrated in certain species, there is limited empirical evidence to support the notion that vessels should expand uniformly throughout the stem with height growth (Weitz et al. 2006; Prendin et al. 2018; Petit et al. 2023). Studies that commonly included the analyses of vertical patterns of wood anatomical traits were restricted to only a few outermost tree-rings at different points

along the main stem (Anfodillo et al. 2006; Petit et al. 2010; Pfautsch et al. 2018; Williams et al. 2019) or branches and petioles (Chen et al. 2012; Ray and Jones 2018). The presence of tip-to-base widening intraspecific variability is an essential prerequisite for empirically testing the adaptive versus non-adaptive hypothesis where natural selection narrows a wider field of evolutionary possibilities (see Figure 2 in Olson et al. 2021).

In this work, we evaluated the consistency of theoretical predictions of vessel widening function in *Fagus sylvatica* L., a diffuse-porous tree species with wide niche across Palearctic temperate forests. Our primary objectives were to investigate: (i) whether the widening exponents of this tree species are consistent with the theoretical predictions of the WBE model and (ii) whether the scaling exponent remains invariant with age, size and growth environment. Various hypotheses can be conceptualized regarding the anatomical changes a tree undergoes during its growth to counteract the effects of height increase: (i) uniform tip-to-base vessel widening (β) with height growth (Prendin et al. 2018), but with the allometric constant (α) increasing with tree height (Olson et al. 2014); (ii) tip-to-base vessel widening not being ontogenetically stable, but with the scaling exponent (β) increasing with tree height, resulting in a slight increase in vessel diameter for a given tree height (Rosell et al. 2017); and (iii) both tip-to-base vessel widening (β) and the allometric constant (α) remain relatively constant with height growth (Prendin et al. 2018; Petit et al. 2023) (see Fig. 1). To test these hypotheses, we have generated a comprehensive dataset encompassing the within-tree variation in vessel diameter. This extensive dataset was constructed through a retrospective reconstruction of the height growth history of 10 mature *F. sylvatica* L. trees, which were collected from two distinct sites in the Italian Apennines, characterized by contrasting climates. Our sampling strategy involved measuring ring-level vessel diameters at multiple positions along the stem, from the pith to the bark. This meticulous approach allowed us to capture the full range of variation in vessel diameter within each tree, resulting in a robust and detailed dataset.

Materials and methods

Study sites and plant material

Plant material came from two selected sites along the Italian peninsula characterized by different climatic conditions. The first site is an even-aged *F. sylvatica* stand in the Abetone forest (Northern Apennines, Italy, 44.10 N, 10.70 E; 1300 m a.s.l.; hereafter Site1) characterized by a perhumid climate with 2046 mm of annual precipitation and a mean annual temperature of 7.8 °C (1981–2010 period). The second even-aged *F. sylvatica* site is in Southern Italy (Serra San Bruno, Southern Apennines; 38.56 N, 16.29 E; 1050 m a.s.l.; hereafter Site2), where the climate is typically Mediterranean with hot dry summers and predominantly winter rainfall; the annual precipitation is 1706 mm and the mean annual temperature is 11.1 °C (1981–2010 period).

Five dominant *F. sylvatica* trees for each site were felled from the study sites and measured for their total height (Table S1 available as Supplementary data at *Tree Physiology* Online). Part of the selected plant material come from previous work (Rita et al. 2020). We reconstructed the apex-to-tree base axial trend within each tree ring to provide an annual resolution the variability of xylem anatomical traits along the stem axis. For each tree, eight transversal stem

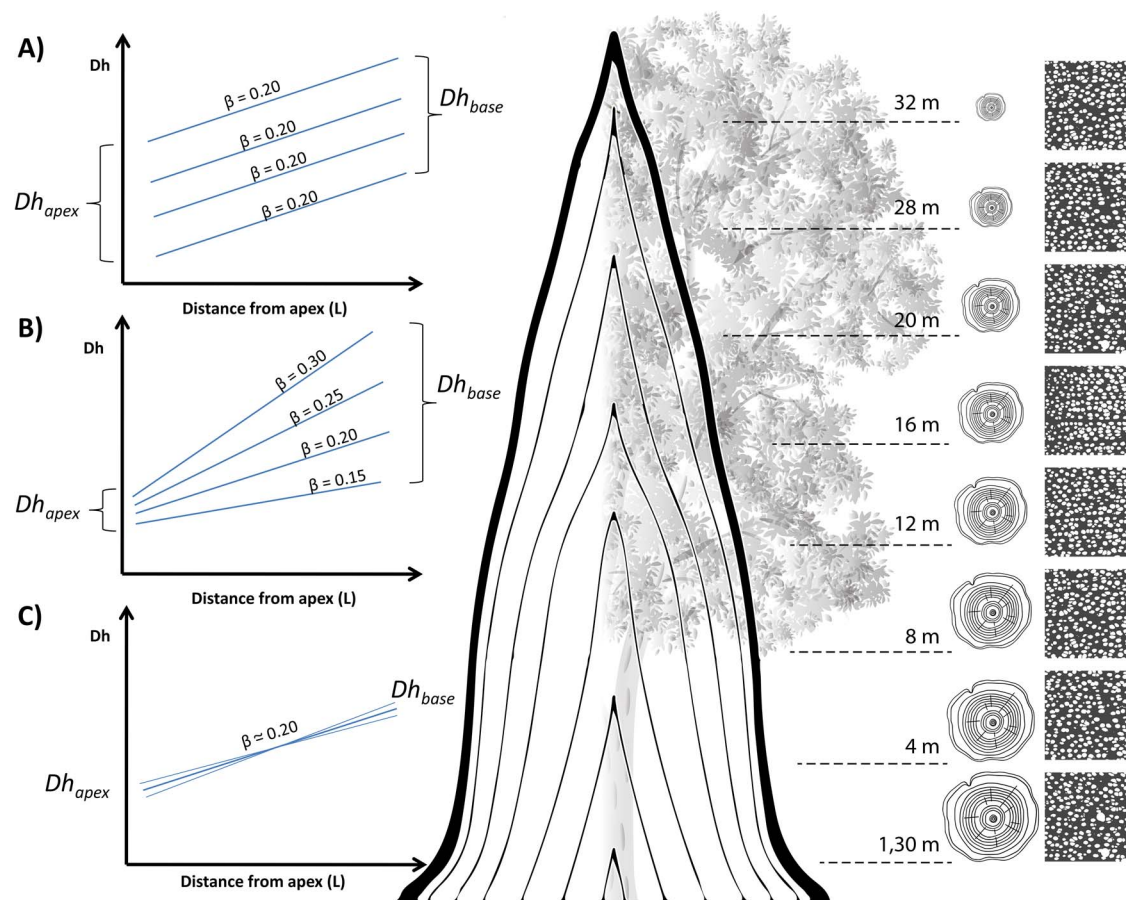


Figure 1. Scheme of the sampling protocol used to reconstruct the axial trend from apex to tree base within each ring. Eight stem discs were harvested at intervals of 1.30, 4, 8, 12, 16, 20, 28 and 32 m along the heights of eight trees (see Table S1 available as Supplementary Data at *Tree Physiology* Online). The annual stem elongation rate was calculated by linearly interpolating the distance between adjacent discs and dividing it by the difference in age between neighboring discs. For each ring, the distance (L) from the stem apex was calculated as the difference between the reconstructed tree height and the distance from the ground. On the left the conceptualized hypotheses concerning the vessel diameter-stem length relationship: (A) uniform tip-to-base vessel widening (β) occurs with height growth, while the allometric constant (α) increases proportionally with tree height; (B) tip-to-base vessel widening is not consistently stable over ontogeny, yet the scaling exponent (β) shows an increase with tree height, leading to a slight adjustment in vessel diameter for a given tree height; (C) both tip-to-base vessel widening (β) and the allometric constant (α) remain relatively consistent as tree height increases. The background tree design is by Freepik.

discs were taken at eight different heights along the main stem i.e. 1.3, 4.0, 8.0, 12.0, 16.0, 20.0, 28.0 and 32.0 m from the base (Fig. 1). In the lab, the width of tree-rings was first measured to the nearest 0.01 mm using a tree-ring measuring system (LINTAB 6 coupled with TSAP-Win Scientific software, Rinntech, Heidelberg, Germany) and then analyzed using COFECHA software (Holmes 1983) to check for cross-dating errors. Further details of stand characteristics, sampling and cross-dating are described in Gentilesca et al. (2018). The retrospective reconstruction of annually resolved height growth rates was generated by stem analysis by means of ring-width data sampled from successive sections along the stems with the ‘IncrementR’ package (Kašpar et al. 2019) in the R statistical environment (R Core Team 2021). The annual height growth rate between two successive stem discs was based on a linear interpolation of their axial distance by the difference in tree-ring counts (Prendin et al. 2018). Accordingly, the total tree height in each year was reconstructed as the height of the last stem disc plus the annual linear growth rate toward the next disc multiplied by the number of years since the last stem disc was reached (i.e. cambial age of the outermost tree ring from the last stem disc). For each site, mean annual temperatures and precipitations were

obtained from the 30-arcsecond resolution data developed by Brunetti et al. (2014) and Crespi et al. (2018), respectively, as extensively detailed in Gentilesca et al. (2018).

Preparation of woody samples

For each collected disc, one radial strip (1 cm wide) running from the bark to the pith was selected to analyze the total radial growth. Samples were first checked to exclude reaction wood, eccentricity or wounding (Jourez et al. 2001, Kašpar et al. 2019) and then radial woody samples were split into 3–4 cm length pieces for processing. After that, anatomical micro cross-sections (15–20 μm of thickness) were cut with a sliding microtome (Microm HM 400, Thermo Sci., Walldorf, Germany), stained with Safranin (1%) and Astra Blue (2%), dehydrated with ethanol and fixed on permanent slides with Eukitt mounting solution (Kindler GmbH, Freiburg, Germany). Digital images were captured with an integrated digital camera (DCM300, ScopeTek) installed on a light microscope (Zeiss Axiophot, Carl Zeiss Microscopy, Jena, Germany). Overlapping images of the whole micro-section were stitched together with Image Composite Editor software (ICE 2.0.3, Microsoft Corp., Redmond, WA, USA).

Quantitative wood anatomy

The images were processed using image-analysis software ImageJ (National Institutes of Health, Bethesda, MD, USA) which allowed measurement of tree-ring lengths and the anatomical features of vessels inside all tree rings. A semi-automated procedure of image analysis was utilized to ascertain the x and y coordinates of the centers of each vessel, as well as their lumen areas. A manual correction was necessary to exclude non-vascular elements or include vessels that had not been selected automatically. Briefly, digital images were converted from 24-bit color in a threshold binary image (mask) in which only the vessel lumens were kept. Before any measurement, the images of all micro-sections were calibrated from a scale bar of known length. For each tree ring, a chosen surface ($\text{Area} = \text{TRW} * l$, where TRW is the tree-ring width and $l = 2$ mm the tangential length) was analyzed for the xylem vessel lumen cross-sectional area (A). Vessel area was converted to diameter (D) assuming circularity of vessels, where

$$D = \sqrt{\frac{4 \cdot A}{\pi}}$$

This transformation allows partially excluding the influence of possible large true tracheids that may have been measured. Based on the vessel contribution to hydraulic conductance, we calculated the hydraulically weighted mean diameter (D_h) for each ring (Tyree and Zimmermann 2002):

$$D_h = \left(\frac{1}{n} \sum_{i=1}^n D_i^4 \right)^{\frac{1}{4}}$$

In total, more than one and a half million xylem vessels were measured. Then, for each tree ring, we calculated the average vessel size (A_{av}), the vessel density (D_v), the theoretical hydraulic conductivity (K_{theo}) and vessel composition (S). The vessel density (D_v) was estimated as the number of vessels per unit of surface area, while the vessel composition (S) was calculated as the ratio between A_{av} and D_v , according to Zanne et al. (2010). The xylem-specific specific hydraulic conductivity (K_s) was estimated according to the modified Hagen-Poiseuille equation reported by Tyree and Ewers (1991, their Eq. (4)):

$$K_s = \frac{\pi \cdot \rho}{128 \cdot \eta \cdot S_i} \sum_{i=1}^n D_i^4$$

where ρ and η are the density and dynamic viscosity of water at 20 °C, respectively, S_i is the ring surface (i.e. tree-ring width * 2 mm), n is the number of vessels per unit of surface area and D is the vessel diameter.

Statistical analyses

To examine multivariate associations between variables, including categorical and continuous variables, we carried out ordinary principal component analysis (PCA) using the *PCAmix* function from the R package *PCAmixdata* (Chavent et al. 2017) in R environment. Entered variables were the tree-ring width (TRW), the hydraulically weighted vessel diameter (D_h), the vessel density (D_v), the specific hydraulic conductivity (K_s), the distance from the apex (D_{apex}), the vessel composition (S) and the cambial age (Age). The study site was set as factor variable into the analysis.

The allometric relationships between the measured traits were analyzed using power scaling model $D_h = \alpha \cdot L^\beta$, where α is the allometric constant and β the scaling exponent. Model parameters were estimated using the standardized major axes (SMAs) with the *smartR* package (Warton et al. 2012). All variables underwent log10 transformation before analysis to satisfy the assumptions of normality and homoscedasticity and to better capture the functional implications of conduit diameter variation (e.g. Kerkhoff and Enquist 2009). This analysis was performed on a maximum common time span and based on data from a moving window of three neighboring tree rings shifted by one to increase the number of axial points and increase the explained deviance of each iteration.

The variability of the α and β coefficients with tree growth was examined using a dual approach, which involved the application of two distinct models for each of the selected predictors. Specifically, the influence of cambial age (Age) and annual height increment (H_{incr}) on the variability of both α and β was initially assessed through a linear mixed-effects approach, incorporating tree ID as a random term. The estimation of parameters in linear mixed-effects models utilizing restricted maximum likelihood (REML) was accomplished using the *lmer* function within the *lme4* package (Bates et al. 2015) in the R environment. We then optimized the random-effect structure of the model testing if including extra random-effects terms for tree ID improved the fit of the model; different random structures were then compared through a Likelihood Ratio Test (LRT). Statistical significance ($P < 0.05$) and Satterthwaite approximation for degrees of freedom were obtained from the *lmerTest* package and confidence intervals of the estimates were computed using the Wald estimation method.

Additionally, we fit linear quantile mixed models to further explore relationships between variables outside of the mean of the data. This model encapsulates a wider quantile (τ) range (from the fifth to the 95th percentile) of the outcome distribution, representing the conditional quantiles of a dependent variable as a linear function of the explanatory variables (R package *lqmm*, v.1.5.8, Geraci 2014). A 95% bootstrap confidence interval for the interquartile regression coefficients was computed with a bootstrap approach (100 replication).

Finally, we integrated all potentially relevant variables, including ontogenetic (i.e. tree age, height and stem diameter increment) and climatic factors (annual temperature and precipitation), into a comprehensive linear mixed model. This model aimed to elucidate the variation in both the allometric constant and the scaling exponent of $D_h \propto L$. The models incorporated tree cambial age (Age), annual height increment (H_{incr}), annual increment of stem diameter (DBH_{incr} , at breast height), site-specific annual average temperature ($Temp$, °C) and cumulated annual precipitation ($Prec$, mm) as fixed effects. Following Zuur et al. (2009), the most parsimonious models were selected using the *lme4* R package (Bates et al. 2015) starting with a saturated model where the fixed component contained all explanatory variables with all possible interactions. Before analysis, all terms were square-root transformed to achieve normality assumption; then all fixed terms were centered and scaled to improve parameter estimates and allow direct comparisons of the regression coefficients. Nested study site and tree ID were included as random variables. Subsequently, we fine-tuned the random-effect configuration of the model by assessing whether the incorporation of random slopes for site ID and tree ID enhanced the model's fit. Different random structures were

compared using an LRT. When comparing saturated models that varied in their random structure but not fixed effects, the models were fit using REML to avoid biased estimators for the variance terms. The final models presented here contains only very limited collinearity ($VIFs < 1.5$). For all models, marginal and conditional R^2 were calculated to examine the variation explained by fixed and fixed plus random factors, respectively, using the *r.squaredGLMM* function in the *MuMIn* package (Barton and Barton 2015). The residual diagnosis was performed to check the normality and homoscedasticity model assumptions.

To quantify the proportion of variance explained by fixed and random terms we partitioned the variance into four components, i.e. variance attributable to fixed terms, variance attributable to random terms and residual variance using the *r2mlm* R package (Shaw et al. 2023). Then, the standardized regression coefficients and the contribution of fixed effects to the variance of dependent variables was computed via *partR2* (R package *partR2* v. 0.9.1, Stoffel et al. 2021) using 1000 parametric bootstrap iterations to calculate 95% confidence intervals of estimates. The within-tree and between-tree variability of α and β coefficients as trees grow taller was tested by estimating the repeatability at both the tree (ID) and site levels. Adjusted repeatability estimates after controlling for fixed effects were obtained using the package *rptR* (Stoffel et al. 2017), all with a Gaussian distribution, using 1000 parametric bootstrap iterations and 100 permutations. The statistical significance of repeatability estimates was inferred from whether confidence intervals included zero.

Results

The first two axes of PCA exploring the interactions between the investigated traits explains 42.7% of the total variance in the data set (Fig. 2a). The first axis is strongly (i.e. PCA score > 0.6) and positively associated with most wood anatomical traits (including D_b , K_{theo} and S) and negatively with D_v . The tree age correlates best with the second axis and negatively associated with the tree-ring width (TRW). Some common patterns of average vessel area (A_{av}), average vessel density (D_v) and vessel lumen composition (S) appeared along the stem length in both study sites (Fig. 2b, c and d). Particularly, A_{av} and S decrease with distance from the stem base while D_v increases. The average vessel area shows more than a two-fold reduction from stem base to top, despite an unusual hump-shaped pattern at breast height, particularly noticeable at Site1. In contrast vessel density there is a sharp increase in the number of vessels along the xylem pathway from 16 m height. Accordingly, the average vessel area shows an increasing pattern with cambial age across the study sites, while vessel density tends to decrease with cambial age (Fig. 3d and e).

An analysis of xylem traits scaling along the stem axis reveals that the power function ($y = a \cdot L^\beta$) provides the best fit to the data (Fig. 3). The hydraulic diameter (D_b) of pooled data per site scaled with the distance to apex reconstructed at annual resolution with scaling exponents β of 0.20 and 0.21 for Site1 and Site2, respectively (model statistics are reported in the Table S2 available as Supplementary data at *Tree Physiology* Online). The vessel density (D_v) scaled with scaling exponents β of -0.24 for Site 1 ($R^2 = 0.24$, $P < 0.001$) and -0.26 for Site 2 ($R^2 = 0.38$, $P < 0.001$) (Fig. S4 available as Supplementary data at *Tree Physiology* Online).

Regarding the D_b – L relationship, the β values exhibit a range of variability spanning from 0.10 to 0.36, encompassing the 95% of the sample distribution. Meanwhile, 50% of the values fall within the range of 0.19 to 0.27, with a median of 0.24. Concerning the allometric constant α , the median value is -4.47 . The range extends from -5.51 to -3.71 for the 95% of the sample distribution and from -4.88 to -4.33 for the 50% of the distribution (Fig. S2 available as Supplementary data at *Tree Physiology* Online). This indicates a considerable range of variability in β and α values among individuals. Notably, for certain cases (i.e. specific annual growth rings), a significant portion of the sampled trees exhibit high values, namely outliers i.e. values of β greater than 0.4 and α less than -6 .

All the models we run agree that no significant trends of β and α exists with respect to Age and H_{incr} (Fig. 4, Table S3 available as Supplementary data at *Tree Physiology* Online). For both scaling parameters, their mean values and percentiles are not influenced by cambial age and annual height increment, with marginal R-squared values well below 1%. However, the conditional R-squared values indicate a pronounced contribution of individual variability in explaining the total variance, i.e. significant between-tree variation (Table S3 available as Supplementary data at *Tree Physiology* Online).

The models that included all potential predictors of the variability in β and α did not show any significant patterns (Fig. 5 and Tables S4 and S5 available as Supplementary data at *Tree Physiology* Online). Although the percentage of total variance explained by both models was quite high (for the β model, R-squared equals 0.70; for the α model, R-squared equals 0.61), the variance partitioning highlighted that only 13% of β variability and $< 10\%$ of α variability can be attributed to fixed factors. This indicates that most of the variability is attributable to random factors, which pertain to differences between and among individuals and between sites (34% and 30% of the total explained variance for β and α , respectively). Upon detailed examination of the variance explained by the random component, we observed that the component most significantly influencing the variability of β and α is almost exclusively attributable to differences among individuals (LRT P -value < 0.001). In contrast, the differences between sites did not show significant contribution (LRT P -value > 0.05 , Fig. S6 available as Supplementary data at *Tree Physiology* Online). The within-individual variability is an equally significant component of variance as the between-individual variability, accounting for over 56% and 63% of the total explained variance for β and α , respectively. We are aware that due to potential inter-annual variability of growth rates, the precision in the estimate of annual stem elongation rate likely decreased with tree age (due to lower inter-disc distance toward the stem base and likely faster growth commonly occurring during the early ontogeny) and we do not exclude the potential impact this may have had on biasing the patterns we observe, particularly in certain years.

Discussion

In this study, we aimed to characterize axial variation of vessel diameter within *F. sylvatica* trees to assess the consistency of predicted tip-to-base conduit widening values with distance from the tree apex. To do this, we analyzed an unparalleled dataset comprising records of long-term xylem anatomical

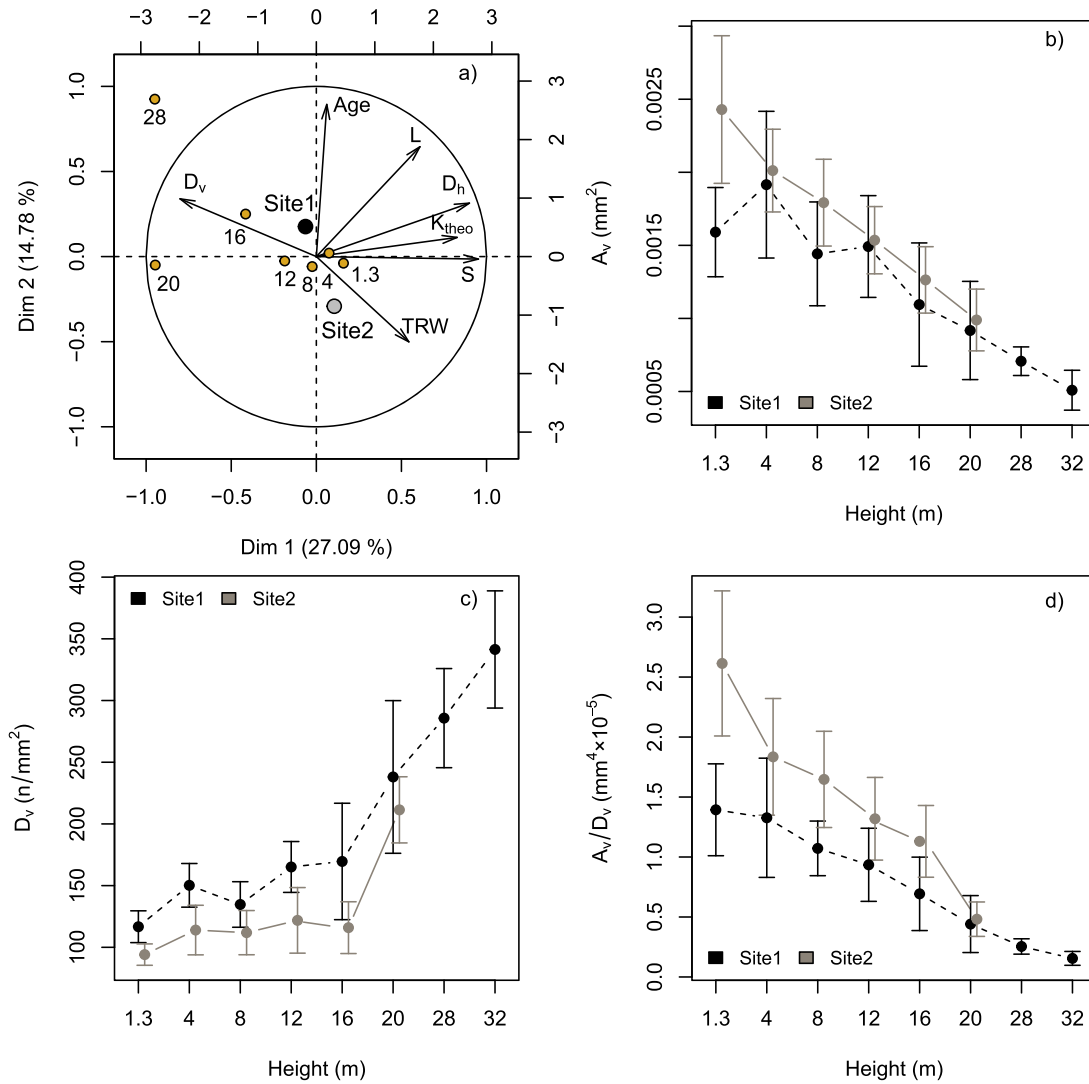


Figure 2. Biplot of the first two axes of the PCA output (panel a). The pattern of average vessel size (A_{av}), vessel density (D_v) and vessel lumen composition ($S = A_{av}/D_v$) for the common tree outermost rings along with stem cross-section height (panels b, c and d). Each data point represents the mean value of different sampling heights, while whiskers represent the mean \pm standard deviation of the mean. TRW, tree-ring width; S, vessel lumen composition; Age, cambial age; D_h , hydraulically weighted vessel diameter, D_v vessel density; K_s , specific hydraulic conductivity; L, distance from the stem apex.

series from different heights along the stems generated through a retrospective reconstruction of the height growth history of 10 mature trees. The negative relationship between vessel density and vessel diameter, consistently observed in our sampled trees, is a well-established phenomenon across woody plants and angiosperms where vessels become smaller with height, leading to increased density (Petit et al. 2010; Lechthaler et al. 2019b). Accordingly, Olson et al. (2020) unveiled a remarkably strong correlation between vessel diameter and density, where vessel density explains a third of the total variation in vessel diameter. This phenomenon occurs because wider vessels occupy a greater proportion of cross-sectional area of the stem than narrower vessels, geometrically resulting in the inverse relationship between vessel diameter and density along the stem. The distinctive pattern of vessels to narrow at the base of the stem, as observed for Site1 (Fig. 2b), has also been documented in tropical tree species (James et al. 2003; Dória et al. 2019; Li et al. 2019) and even in *Eucalyptus* spp. (Petit et al. 2010; Pfautsch et al. 2018). This trend deviates from the prevailing pattern of continuous

vessel widening from the tip to the base of the tree. While we lack substantial evidence to draw similar conclusions for our angiosperm species, the reasons for basal narrowing of vessels warrants further investigation. Some hypotheses put forth include considerations of xylem construction costs (e.g. Mencuccini et al. 2007) or rather the alleviation of mechanical stress (e.g. Gartner 1995) or invoke a trade-off between fluid dynamic resistance and carbon cost of the conducting system (Koçillari et al. 2021).

Predictability of vessel diameter change with tree height

The results from our long-term stem anatomical series strongly emphasize that vessel diameter follows a predictable pattern with distance from the stem apex. This finding robustly supports the hypothesis that, with height growth, trees do not alter their axial configuration (both α and β in the equation $D_b = \alpha \times L^\beta$) to compensate for hydraulic limitations imposed by tree height during growth. Our

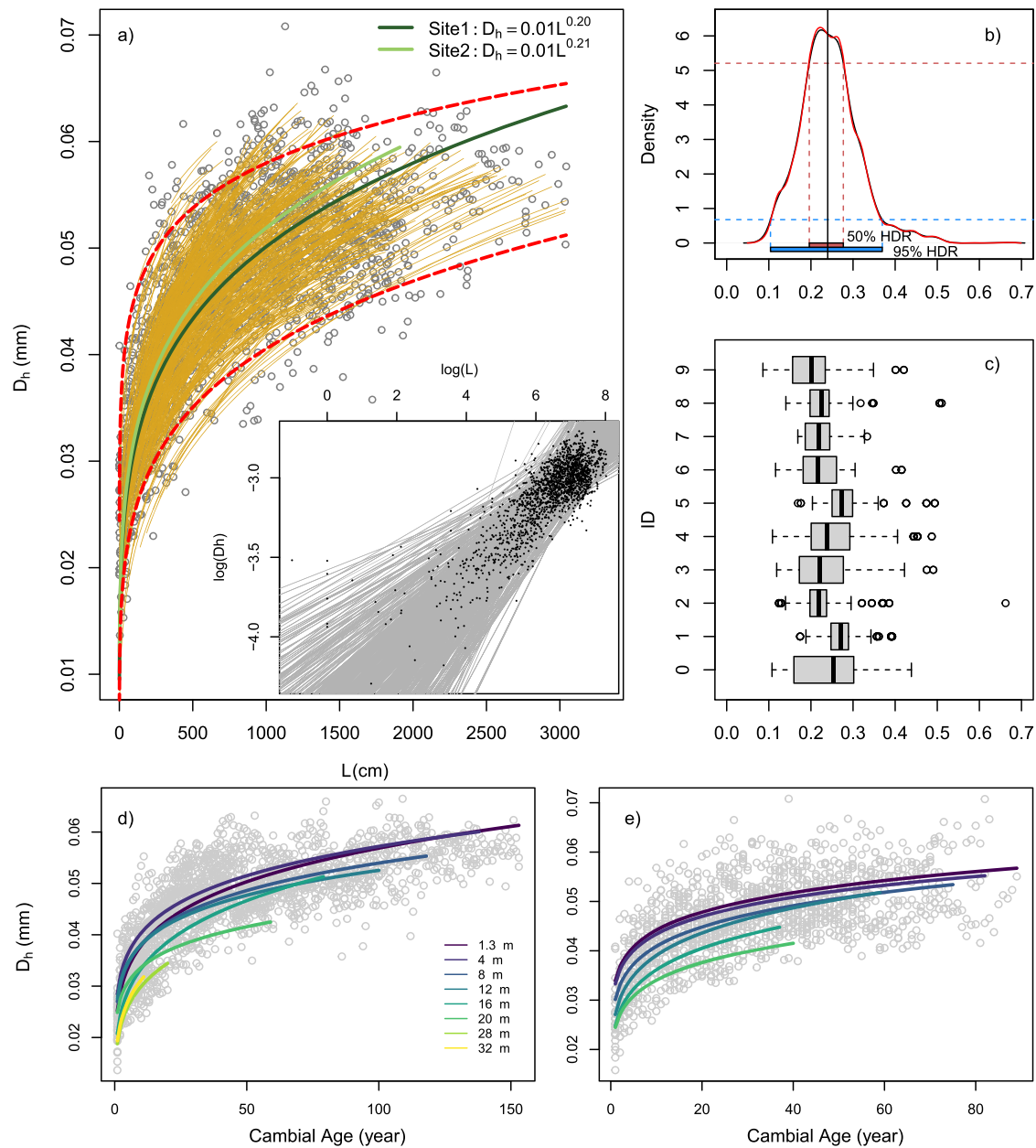


Figure 3. Axial variation of hydraulic vessel diameter (D_h) versus distance from the tree top (L) (a). The thin lines are the predicted value of linear log-log models for each cambial age; the thick lines are the predicted value for Site1 ($\alpha = -4.44$, $\beta = 0.20$, $R^2 = 0.71$, $P < 0.001$) and Site2 ($\alpha = -4.42$, $\beta = 0.21$, $R^2 = 0.55$, $P < 0.001$), respectively. The dashed lines represent the fifth and 95th percentiles. Insets show log-log scaling between variables. Estimated univariate density distribution of β scaling exponents with highest density regions (HDR; red 50% and blue 95%) displayed; the vertical full line corresponds to the median value 0.24 (b). Box plots showing β scaling exponent variability for sampled trees. Each box represents the 75th to 25th percentiles and the line inside the median; the upper and lower marks are the largest to smallest observation values, which are less than or equal to the upper and lower quartile plus 1.5 the length of the interquartile range; the circles outside the lower-upper mark range are outliers (c). Radial variation of hydraulic vessel diameter (D_h) versus tree cambial age for Site1 (d) and Site2 (e). The thin lines are the predicted value of linear log-log models for collected stem disk.

finding that hydraulic vessel diameter increases with distance from the tree apex is consistent with existing knowledge and supports the hypothesis that the widening of xylem vessels is a result of natural selection, aimed at minimizing the negative impact of path length on resistance along the conductive pathway (Anfodillo et al. 2013). Whatever the mechanisms regulating the vessel diameter dimensions along the stem, i.e. turgor (Woodruff and Meinzer 2011; Cabon et al. 2020) or hormones (Anfodillo et al. 2012; Johnson et al. 2018), such tip-to-base widening profiles are observed

in over a hundred species regardless of phylogenetic affinity (including ferns, clubmosses, horsetails and spikemosses), plant heights, growth habit or climate (James et al. 2003; Anfodillo et al. 2006; Mencuccini et al. 2007; Petit et al. 2010, 2023; Williams et al. 2019; Olson et al. 2014; Yang et al. 2021, but refer to Olson et al. 2021 for a comprehensive review). The observed axial widening pattern of D_h within the *F. sylvatica* stem appears to be a result of natural selection to favor a mechanism that mitigates the decline in hydraulic conductance with increasing path length. This concept is

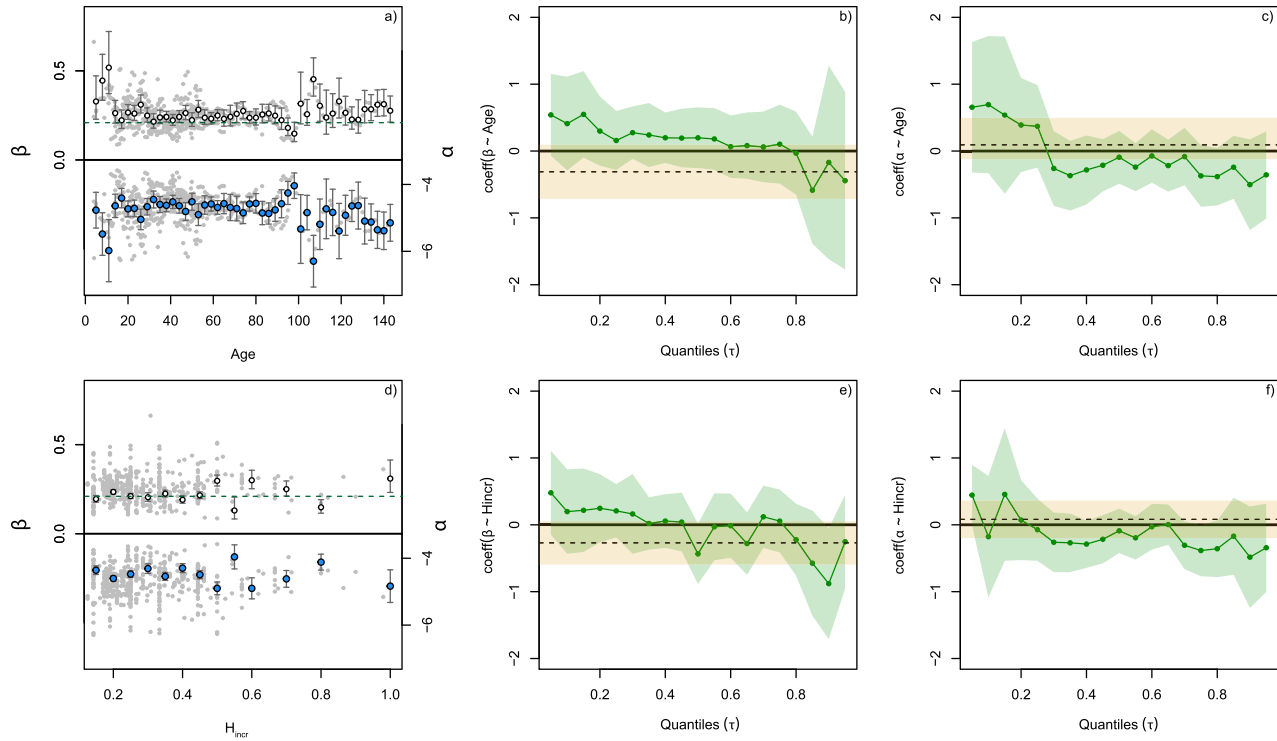


Figure 4. Average values (depicted as points) along with 95% confidence intervals (illustrated as error bars) of the scaling exponent β (indicated by empty dots) and the allometric constant α (on a log scale, represented by full dots). The average values encompass pooled data from all individuals categorized by age (a) and annual height increment rate (d). Individual data can be found in Fig. S5 available as Supplementary data at *Tree Physiology* Online. The background dots represent the input data and the dashed horizontal lines represent $\beta = 0.2$. The slope coefficient (shown as dashed lines) and its 95% confidence interval (shaded area) of the estimated linear mixed model regression of the scaling exponent β (b, e) and the allometric constant α (c, f). These regressions are presented in relation to the tree cambial age (*Age*, upper panels) and annual height increment (H_{incr} , lower panels). The full lines and points indicate the slope of the estimated linear mixed quantile regression with respect to the τ^{th} quantile τ (represented by full circles, each corresponding to the fifth quantile). The shaded area represents the 95% confidence interval (obtained through 1000 replicate bootstrap iterations) for the quantile estimates.

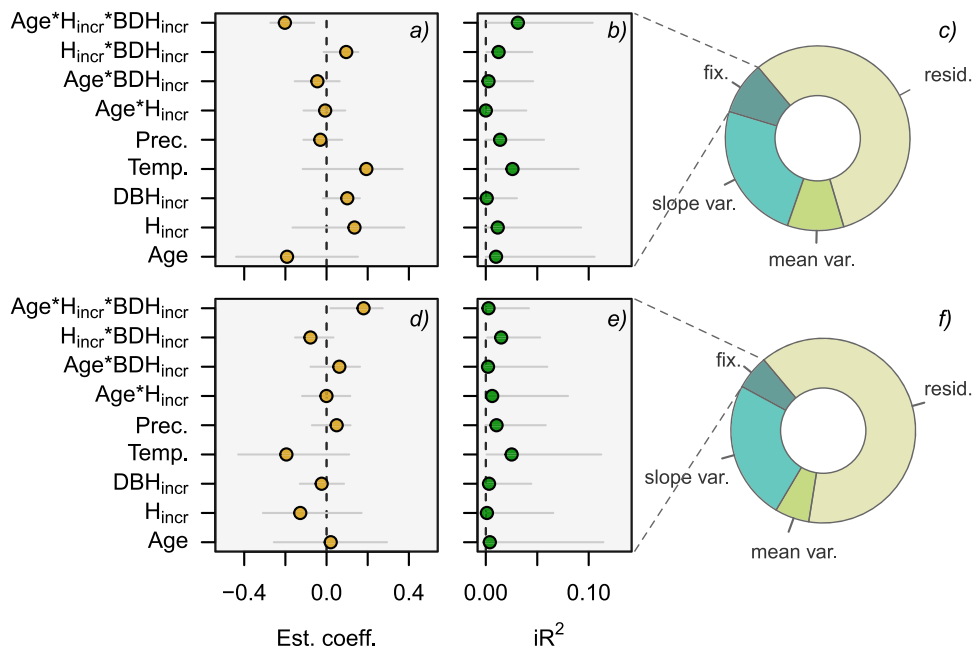


Figure 5. Estimated coefficients (points) and their 95% confidence intervals of the linear mixed model for β (upper panels) and α (lower panels) (a, d). Cambial age (*Age*), annual height increment (H_{incr}), annual stem diameter increment (DBH_{incr}), annual average temperature (*Temp.*) and cumulated annual precipitation (*Prec.*), * denotes variable interaction. Inclusive iR^2 defined as the variance explained by a predictor irrespective of covariances with other predictors (b, e). Variance components of the linear mixed effects models (c, f) explained by fixed variables (fix.), random variation among trees and between sites (mean var. and slope var.) and the within-tree residual variability (resid.).

consistent with the original theories proposed by the WBE model and the widened pipe model (West et al. 1999; Enquist et al. 2000; Anfodillo et al. 2006; Koçillari et al. 2021) and fully consistent with the patterns found in Petit et al. (2023) for the same species, highlighting that the observed widening pattern minimizes, but does not fully eliminate, the path length resistance.

In our dataset, the power scaling exponent between the hydraulically weighted vessel diameter (D_h) and the distance from the stem apex (L) mostly fell inside the range 0.15 to 0.33 values reported for various tree species (Anfodillo et al. 2006). Moreover, β values reported for both our sites remarkably match with the predictions of hydraulic optimality models, specifically, the expectation of a vessel diameter-stem length exponent of 0.2 as supported by empirical measurements by Anfodillo et al. (2006). When compared with other studies on *F. sylvatica* species (i.e. $\beta = 0.23$ in Petit et al. 2023), we detected no significant difference in the β scaling exponent, as indicated by the overlapping 95% confidence intervals.

In some cases, we observed widening values significantly exceeding the predicted threshold (i.e. $\beta = 0.31$). This phenomenon, referred to as overwidening (“overtapering” sensu Anfodillo et al. 2006), in vessel structure, has also been documented in other species (e.g. *Fraxinus excelsior* in Anfodillo et al. 2006 and in *Eucalyptus regnans* in Petit et al. 2010) and partly attributed to trees with elevated height increment. However, our analyses did not support the hypothesis that high degrees of vessel widening are frequently linked with trees displaying fast height growth in their early ontogeny.

Nevertheless, despite the variability in the β exponent within species and even within the same individual (see discussion below), the optimality predictions with respect to widening rates, as supported by empirical evidence, converge on the idea of the “just right” exponent (as per Olson et al. 2021), corresponding to values close to 0.2. Values of β close to this threshold, resulting in hydraulic resistance remaining relatively constant with increasing stem length, are likely to be favored by natural selection over other patterns of axial variation of vessel traits as vessels offer an efficient conductivity rate without excessively increasing the risk of embolism or metabolic cost.

The D_v – L relationship (Fig. S4 available as Supplementary data at *Tree Physiology* Online) closely mirrored the D_h – L relationship in that it was well described by the similar power trajectories for all trees. While longer stem length corresponds to higher D_h , the negative relationship between D_v and L was expected given the well-documented geometrical relationship between D_h and D_v (Petit et al. 2010, Olson et al. 2020).

Tip-to-base vessel widening remains stable with height growth

Our results, based on detailed anatomical measurements at the individual level, explicitly demonstrate that vessel widening remains consistent throughout each year of growth, from the ring apex to the stem base. The fact that allometric parameters α and β remain unchanged as an individual tree grows taller has limited but valuable supporting evidence to date, with only a few studies, including Weitz et al. (2006) on a specimen of *Fraxinus americana*, Prendin et al. (2018) on eight specimens of *Larix decidua* and Petit et al. (2023) on a specimen of *F. sylvatica* and *Picea abies*, providing confirmation. Despite the expected changes in xylem structure

as trees grow, the slope of the relationship D_h – L remains essentially constant, suggesting strong developmental control over axial design. This suggests that the vascular system does not adjust to higher cambial age and tree height by modifying its axial scaling components. This lack of increase in either stem apex vessel diameter or tip-to-base widening rate means that the observed widening pattern minimizes, but does not fully eliminate, the path resistance length. However, Petit et al. (2023) have recently shown that while species-specific differences would alter the effects of these residual path length influences at the tree-ring level, the contribution of inner sapwood rings to the total xylem conductance becomes crucial in effectively mitigating the hydraulic limitations imposed by tree height on leaf-specific conductance.

Given the negative relationship between β and α (Fig. S7 available as Supplementary data at *Tree Physiology* Online), we expected that α of the within-individual tip-to-base widening profile would remain constant as an individual grows taller, indicating an absence of pattern of α with height growth. This is consistent with other intraspecific investigations that report only negligible variation with ontogeny, such as Prendin et al. (2018); Williams et al. (2019) and Petit et al. (2023). However, these results are not in line with interspecific outcomes that estimate mean vessel diameter at the distal-most twig from the base becomes predictably wider across angiosperms (Echeverría et al. 2019, Olson et al. 2014, 2020, see below discussion on leaf size effect).

We observed that the widening vessel rate of *F. sylvatica* remains consistent between sites with contrasting climate. This means that the basal vessel size–tree height relationship is chiefly influenced by tree height rather than by climate. This finding is consistent with studies conducted on other tree species across precipitation gradients, which observed no significant changes in the slope and intercept of tip-to-base vessel widening profiles (e.g. seven *Acacia* spp. in Lechthaler et al. 2019b; two *Cedrela* spp. in Chambers-Ostler et al. 2023; *Nothofagus antarctica* in Fajardo et al. 2020, although the latter did not measure axial profiles of xylem vessels). While there were minor differences reported in *Fraxinus* trees growing in soils with varying moisture retention (Kiorapostolou and Petit 2019), temperate conifers have consistently exhibited a constant tip-to-base vessel widening regardless of nutrient availability, temperature (Coomes et al. 2007) and even experimental manipulation of CO₂ concentration and soil temperature (Prendin et al. 2018). This suggests that tree size is a more reliable predictor of basal vessel size than climate across various tree species and sizes, as demonstrated by Olson et al. (2014), where stem length explained 63% of the total variation in vessel diameter. However, it is important to note that climate-related variables can still affect intra- and interannual xylem vessel patterns, but these effects should be considered in the context of the causal relationship between plant size and vessel diameter, as suggested by Rosell et al. (2017).

Another piece of evidence supporting the consistency of the widening coefficients between sites emerged when we tested the temporal correlation among individuals from the same site. In accordance with a key assumption of dendrochronology, if the local climate had a predominant effect, we would have expected trees growing in the same site and climate to exhibit similar patterns in the examined traits (Fritts 1976). However, the temporal correlation tests conducted among individuals from the same site revealed only partial or

contrasting significant Pearson correlation coefficient, indicating the absence of common patterns among individuals (Table S6 available as Supplementary data at *Tree Physiology* Online). This further corroborates the legacy of developmental history of individual tree in the stand (Olson et al. 2021). Indeed, individual development is intricately linked to both common site-specific factors (e.g. microclimate, soil, nutrients) and factors driving forest dynamics (competition for resources among trees) that influence phenotypic variation in plant traits. Accordingly, we are aware that certain site-specific factors, such as nutrient availability (Borghetti et al. 2017) and water storage capacity (Tokumoto et al. 2014), possible variability randomly introduced by reconstructing tree height at annual resolution, as well as genetic background (Eilmann et al. 2014), which were not considered in our analysis, may partially affect the interpretation of our results.

We demonstrate that within-tree variation is a substantial, rather than a minor, contributor to the overall variance of the widening exponent. Numerous studies have highlighted that certain species exhibit intra-specific variations in xylem traits in response to site-specific or environmental conditions, while other research has shown limited intra-specific differences (Herbette et al. 2010; Schreiber et al. 2015; Hajek et al. 2016; Baer et al. 2021; Weithmann et al. 2022), although a large body of it does not denote standardized sampling approaches (see Petit et al. 2022 for a critique on this matter). Yet, significant variability in xylem traits can exist within an organism, both along its main plant axis and between its roots and stems (Jacobsen et al. 2018; Prendin et al. 2018; Rodriguez-Zaccaro et al. 2019; Baer et al. 2021). For instance, Baer et al. (2021) investigated intra-organismal variability in xylem traits such as density, biomechanics and water storage within a model angiosperm species, revealing that these variations arise in response to different biomechanical stresses on shoots and roots, as well as varying root-leaf water potential gradients within the plant. This leads to trade-offs within the xylem of a single individual, particularly between biomechanical and water-storage functions. Hence, in response to selective pressures from the surrounding environment, trees can exhibit significant intra-specific and intraindividual differences in xylem traits, potentially leading to systematic variations in the vessel diameter–plant height relationship within the boundaries of developmental possibilities (Olson et al. 2021). Within certain limits, authors concur that the vessel diameter–stem length exponent is not constant, suggesting the presence of systematic developmental variations that allow different slopes and intercepts (Rosell et al. 2017; Olson et al. 2021). Currently, there are emergent hypotheses indicating that features such as leaf phenology, wood density, porosity type and perforation plate type are linked to significant variations in vessel scaling slope and intercept that have adaptive implications (see Olson et al. 2020 for an overview). For example, there is every reason to believe that leaf size could play a crucial role in this context, particularly in determining the diameter of the conductive vessels in the distal parts of the branches (Lechthaler et al. 2019a; Cao et al. 2022), likely influencing the tip-to-base conduit widening profile in the stem. Additionally, some evidence suggests that taller individuals within a species may exhibit slightly lower tip-to-base scaling exponents (Mencuccini et al. 2007; Petit et al. 2008) to balance the need for efficient hydraulic transport with the constraints of carbon cost. Collectively, these studies indicate that there exists room for selection to influence not only narrower but also wider vessels than

typically observed for a given stem length (Olson et al. 2021). Within the framework of vessel scaling, individuals within a population that deviate significantly from the typical scaling pattern, either above or below, are expected to exhibit reduced performance or fitness compared with those individuals that closely adhere to the common scaling pattern (Anfodillo et al. 2016; Anfodillo and Olson 2021). Considering the potential functional significance of this variation, gaining a comprehensive understanding of factors contributing to intra-individual variation in widening exponent is a priority in comprehending how plants adapt and acclimate to climate-related disturbances.

Conclusion

In our study, we explored axial variation in xylem vessel characteristics in a diffuse porous tree species to assess the consistency of theoretical predictions regarding the power scaling widening exponent of the relationships $D_b \propto L$. We examined 10 *F. sylvatica* L. trees from two contrasting climate sites. Although we identified a steady scaling exponent with height growth and between study sites there was still inherent variability in tip-to-base vessel widening among and within individual trees. Our findings emphasize that the primary source of variance in the relationship between tree height and hydraulic vessel diameter is the variation within and between trees. These results highlight our current lack of understanding regarding the origins of variation in the scaling exponent or the y-intercepts, indicating these as critical areas for future research. Given the potential functional importance of this variation, it is crucial to deepen the understanding of factors that contribute to the variation in intraindividual widening exponent in relation to plants' adaptation and acclimation to climate-related disturbances.

Acknowledgments

We thank A. Lapolla (University of Basilicata, Potenza, Italy) for assistance in sampling trees in the field. The authors would like to express their gratitude to the reviewers Gai Petit and Mark Olson for their thoughtful comments and efforts toward improving the manuscript.

Authors' contributions

A.R. designed and conducted the study and wrote the manuscript; O.P. and T.G. carried out the measurements; A.R. and J.T. performed the analysis. All authors contributed to discussing and interpreting the data throughout the study.

Supplementary data

Supplementary data are available at *Tree Physiology* Online.

Conflict of interest

The authors declare no conflict of interest.

Funding

A.R.'s work was supported by the Agritech National Research Center and received funding from the European Union Next-GenerationEU (PIANO NAZIONALE DI RIPRESA E RESILIENZA (PNRR)—MISSIONE 4 COMPONENTE 2, INVESTIMENTO 1.4—D.D. 1032 17/06/2022, CN00000022). This manuscript reflects only the

authors' views and opinions; neither the European Union nor the European Commission can be considered responsible for them. O.P. was supported by the project "Advanced EO Technologies for studying Climate Change impacts on the environment - OT4CLIMA" which was funded by the Italian Ministry of Education, University and Research (D.D. 2261 del 6.9.2018, PON R&I 2014-2020 e FSC) and by the PhD program in "Agricultural, Forest and Food Sciences" at the University of Basilicata, Potenza, Italy.

Data availability

The data and materials that support the findings of this study are available from the corresponding author upon reasonable request.

References

- Anfodillo T, Olson ME. 2021. Tree mortality: testing the link between drought, embolism vulnerability and xylem conduit diameter remains a priority. *Front For Glob Change*. 4:704670. <https://doi.org/10.3389/ffgc.2021.704670>.
- Anfodillo T, Carraro V, Carrer M, Fior C, Rossi S. 2006. Convergent tapering of xylem conduits in different woody species. *New Phytol*. 169(2):279–290. <https://doi.org/10.1111/j.1469-8137.2005.01587.x>.
- Anfodillo T, Deslauriers A, Menardi R, Tedoldi L, Petit G, Rossi S. 2012. Widening of xylem conduits in a conifer tree depends on the longer time of cell expansion downwards along the stem. *J Exp Bot*. 63(2): 837–845. <https://doi.org/10.1093/jxb/err309>.
- Anfodillo T, Petit G, Crivellaro A. 2013. Axial conduit widening in woody species: a still neglected anatomical pattern. *IAWA J*. 34(4): 352–364. <https://doi.org/10.1163/22941932-00000030>.
- Anfodillo T, Petit G, Sterck F, Lechthaler S, Olson ME. 2016. Allometric trajectories and "stress": a quantitative approach. *Front Plant Sci*. 7:1681. <https://doi.org/10.3389/fpls.2016.01681>.
- Baer AB, Fickle JC, Medina J, Robles C, Pratt RB, Jacobsen AL. 2021. Xylem biomechanics, water storage and density within roots and shoots of an angiosperm tree species. *J Exp Bot*. 72(22):7984–7997. <https://doi.org/10.1093/jxb/erab384>.
- Barton K, Barton MK. 2015. Package 'MuMin'. Version. 1(18):439.
- Bates D, Mächler M, Bolker B, Walker S. 2015. Fitting linear mixed-effects models using lme4. *J Stat Softw*. 67(1):1–48.
- Becker P, Gribben RJ, Lim CM. 2000. Tapered conduits can buffer hydraulic conductance from path-length effects. *Tree Physiol*. 20(14):965–967. <https://doi.org/10.1093/treephys/20.14.965>.
- Borghetti M, Gentilesca T, Leonardi S, Van Noije T, Rita A, Mencuccini M. 2017. Long-term temporal relationships between environmental conditions and xylem functional traits: a meta-analysis across a range of woody species along climatic and nitrogen deposition gradients. *Tree Physiol*. 37(1):4–17. <https://doi.org/10.1093/treephys/tpw087>.
- Brunetti M, Maugeri M, Nanni T, Simolo C, Spinoni J. 2014. High-resolution temperature climatology for Italy: interpolation method intercomparison. *Int J Climatol*. 34(4):1278–1296. <https://doi.org/10.1002/joc.3764>.
- Cabon A, Fernández-de-Uña L, Gea-Izquierdo G, Meinzer FC, Woodruff DR, Martínez-Vilalta J, De Cáceres M. 2020. Water potential control of turgor-driven tracheid enlargement in Scots pine at its xeric distribution edge. *New Phytol*. 225(1):209–221. <https://doi.org/10.1111/nph.16146>.
- Cao X, Li Y, Zheng XJ, Xie JB, Wang ZY. 2022. An inherent coordination between the leaf size and the hydraulic architecture of angiosperm trees. *Forests*. 13(8):1287. <https://doi.org/10.3390/f13081287>.
- Chambers-Ostler A, Gloor E, Galbraith D, Groenendijk P, Brien R. 2023. Vessel tapering is conserved along a precipitation gradient in tropical trees of the genus *Cedrela*. *Trees*. 37(2):269–284. <https://doi.org/10.1007/s00468-022-02345-6>.
- Chavent M, Kuentz V, Labenne A, Lique B, Saracco J. 2017. PCAmix-data: multivariate analysis of mixed data. R package version, 3.
- Chen H, Niklas KJ, Sun S. 2012. Testing the packing rule across the twig–petiole interface of temperate woody species. *Trees*. 26(6): 1737–1745. <https://doi.org/10.1007/s00468-012-0742-3>.
- Coomes DA, Jenkins KL, Cole LE. 2007. Scaling of tree vascular transport systems along gradients of nutrient supply and altitude. *Biol Lett*. 3(1):87–90. <https://doi.org/10.1098/rsbl.2006.0551>.
- Crespi A, Brunetti M, Lentini G, Maugeri M. 2018. 1961–1990 high-resolution monthly precipitation climatologies for Italy. *Int J Climatol*. 38(2):878–895. <https://doi.org/10.1002/joc.5217>.
- Dória LC, Podadera DS, Lima RS, Lens F, Marcati CR. 2019. Axial sampling height outperforms site as predictor of wood trait variation. *IAWA J*. 40(2):191–153. <https://doi.org/10.1163/22941932-40190245>.
- Echeverría A, Anfodillo T, Soriano D, Rosell JA, Olson ME. 2019. Constant theoretical conductance via changes in vessel diameter and number with height growth in *Moringa oleifera*. *J Exp Bot*. 70(20): 5765–5772. <https://doi.org/10.1093/jxb/erz329>.
- Eilmann B, Sterck F, Wegner L, de Vries SM, Von Arx G, Mohren GM, den Ouden J, Sass-Klaassen U. 2014. Wood structural differences between northern and southern beech provenances growing at a moderate site. *Tree Physiol*. 34(8):882–893. <https://doi.org/10.1093/treephys/tpu069>.
- Enquist BJ, West GB, Brown JH. 2000. Quarter-power allometric scaling in vascular plants: functional basis and ecological consequences. In: Brown JH and West GB, editors. *Scaling in Biology* (New York, NY, 2000; online edn, Oxford Academic, 31 Oct. 2023). p. 167–198. <https://doi.org/10.1093/oso/9780195131413.003.0010>.
- Fajardo A, Martínez-Pérez C, Cervantes-Alcayde MA, Olson ME. 2020. Stem length, not climate, controls vessel diameter in two tree species across a sharp precipitation gradient. *New Phytol*. 225(6): 2347–2355. <https://doi.org/10.1111/nph.16287>.
- Fritts H. 1976. *Tree rings and climate*. London: Academic Press.
- Gartner BL. 1995. Patterns of xylem variation within a tree and their hydraulic and mechanical consequences. In: *Plant stems: physiological and functional morphology*. San Diego, California: Academic Press, pp 125–149.
- Gentilesca T, Rita A, Brunetti M, Giammarchi F, Leonardi S, Magnani F, Van Noije T, Tonon G, Borghetti M. 2018. Nitrogen deposition outweighs climatic variability in driving annual growth rate of canopy beech trees: evidence from long-term growth reconstruction across a geographic gradient. *Glob Chang Biol*. 24(7):2898–2912. <https://doi.org/10.1111/gcb.14142>.
- Geraci M. 2014. Linear quantile mixed models: the lqmm package for Laplace quantile regression. *J Stat Softw*. 57(13):1–29.
- Hacke UG, Sperry JS, Wheeler JK, Castro L. 2006. Scaling of angiosperm xylem structure with safety and efficiency. *Tree Physiol*. 26(6):689–701. <https://doi.org/10.1093/treephys/26.6.689>.
- Hacke UG, Jacobsen AL, Pratt RB. 2023. Vessel diameter and vulnerability to drought-induced embolism: within-tissue and across-species patterns and the issue of survivorship bias. *IAWA J*. 44(3–4): 304–319.
- Hajek P, Kurjak D, von Wühlisch G, Delzon S, Schuldt B. 2016. Intraspecific variation in wood anatomical, hydraulic and foliar traits in ten European beech provenances differing in growth yield. *Front Plant Sci*. 7:791.
- Herbette S, Wortemann R, Awad H, Huc R, Cochard H, Barigah TS. 2010. Insights into xylem vulnerability to cavitation in *Fagus sylvatica* L.: phenotypic and environmental sources of variability. *Tree Physiol*. 30(11):1448–1455. <https://doi.org/10.1093/treephys/tpq079>.
- Holmes RL. 1983. Computer assisted quality control in tree-ring dating and measurement. *Tree Ring Bull*. 43:69–78.
- Jacobsen AL, Pratt RB. 2023. Vessel diameter polymorphism determines vulnerability-to-embolism curve shape. *IAWA J*. 44(3–4): 320–334.
- Jacobsen AL, Valdovinos-Ayala J, Rodríguez-Zaccaro FD, Hill-Crim MA, Percolla MI, Venturas MD. 2018. Intra-organismal variation in

- the structure of plant vascular transport tissues in poplar trees. *Trees*. 32(5):1335–1346. <https://doi.org/10.1007/s00468-018-1714-z>.
- James SA, Meinzer FC, Goldstein G, Woodruff D, Jones T, Restom T, Mejia M, Clearwater M, Campanello P. 2003. Axial and radial water transport and internal water storage in tropical forest canopy trees. *Oecologia*. 134(1):37–45. <https://doi.org/10.1007/s00442-002-1080-8>.
- Johnson D, Eckart P, Alsamadisi N, Noble H, Martin C, Spicer R. 2018. Polar auxin transport is implicated in vessel differentiation and spatial patterning during secondary growth in *Populus*. *Am J Bot*. 105(2):186–196. <https://doi.org/10.1002/ajb2.1035>.
- Jourez B, Riboux A, Leclercq A. 2001. Anatomical characteristics of tension wood and opposite wood in young inclined stems of poplar (*Populus euramericana* cv “ghoy”). *IAWA J*. 22(2):133–157. <https://doi.org/10.1163/22941932-90000274>.
- Kašpar J, Tumajer J, Treml V. 2019. IncrementR: analysing height growth of trees and shrubs in R. *Dendrochronologia*. 53:48–54. <https://doi.org/10.1016/j.dendro.2018.11.001>.
- Kerkhoff AJ, Enquist BJ. 2009. Multiplicative by nature: why logarithmic transformation is necessary in allometry. *J Theor Biol*. 257(3): 519–521. <https://doi.org/10.1016/j.jtbi.2008.12.026>.
- Kiorapostolou N, Petit G. 2019. Similarities and differences in the balances between leaf, xylem and phloem structures in *Fraxinus ornus* along an environmental gradient. *Tree Physiol*. 39(2):234–242. <https://doi.org/10.1093/treephys/tpy095>.
- Koçillari L, Olson ME, Suweis S, Rocha RP, Lovison A, Cardin F, Maritan A. 2021. The widened pipe model of plant hydraulic evolution. *Proc Natl Acad Sci USA*. 118(22):e2100314118. <https://doi.org/10.1073/pnas.2100314118>.
- Lechthaler S, Colangeli P, Gazzabin M, Anfodillo T. 2019a. Axial anatomy of the leaf midrib provides new insights into the hydraulic architecture and cavitation patterns of *Acer pseudoplatanus* leaves. *J Exp Bot*. 70(21):6195–6201. <https://doi.org/10.1093/jxb/erz347>.
- Lechthaler S, Turnbull TL, Gelmini Y, Pirotti F, Anfodillo T, Adams MA, Petit G. 2019b. A standardization method to disentangle environmental information from axial trends of xylem anatomical traits. *Tree Physiol*. 39(3):495–502. <https://doi.org/10.1093/treephys/tpy110>.
- Lechthaler S, Kiorapostolou N, Pitacco A, Anfodillo T, Petit G. 2020. The total path length hydraulic resistance according to known anatomical patterns: what is the shape of the root-to-leaf tension gradient along the plant longitudinal axis? *J Theor Biol*. 502:110369. <https://doi.org/10.1016/j.jtbi.2020.110369>.
- Li S, Li X, Link R, Li R, Deng L, Schuldt B, Jiang X, Zhao R, Zheng J, Li S et al. 2019. Influence of cambial age and axial height on the spatial patterns of xylem traits in *Catalpa bungei*, a ring-porous tree species native to China. *Forests*. 10(8):662. <https://doi.org/10.3390/f10080662>.
- Meinzer FC, Lachenbruch B, Dawson TE (eds). 2011. Size-and age-related changes in tree structure and function, Vol. 4. Dordrecht, Netherlands: Springer Science & Business Media.
- Mencuccini M, Hölttä T, Petit G, Magnani F. 2007. Sanio’s laws revisited. Size-dependent changes in the xylem architecture of trees. *Ecol Lett*. 10(11):1084–1093. <https://doi.org/10.1111/j.1461-0248.2007.01104.x>.
- Olson M, Rosell JA, Martínez-Pérez C, León-Gómez C, Fajardo A, Isnard S, Cervantes-Alcayde MA, Echeverría A, Figueroa-Abundiz VA, Segovia-Rivas A et al. 2020. Xylem vessel diameter–shoot-length scaling: ecological significance of porosity types and other traits. *Ecol Monogr*. 90(3):e01410. <https://doi.org/10.1002/ecm.1410>.
- Olson ME, Anfodillo T, Rosell JA, Petit G, Crivellaro A, Isnard S, León-Gómez C, Alvarado-Cárdenas LO, Castorena M. 2014. Universal hydraulics of the flowering plants: vessel diameter scales with stem length across angiosperm lineages, habits and climates. *Ecol Lett*. 17(8):988–997. <https://doi.org/10.1111/ele.12302>.
- Olson ME, Soriano D, Rosell JA, Anfodillo T, Donoghue MJ, Edwards EJ, León-Gómez C, Dawson T, Camarero Martínez JJ, Castorena M et al. 2018. Plant height and hydraulic vulnerability to drought and cold. *Proc Natl Acad Sci USA*. 115(29):7551–7556. <https://doi.org/10.1073/pnas.1721728115>.
- Olson ME, Anfodillo T, Gleason SM, McCulloh KA. 2021. Tip-to-base xylem conduit widening as an adaptation: causes, consequences and empirical priorities. *New Phytol*. 229(4):1877–1893. <https://doi.org/10.1111/nph.16961>.
- Petit G, Anfodillo T. 2009. Plant physiology in theory and practice: an analysis of the WBE model for vascular plants. *J Theor Biol*. 259(1): 1–4. <https://doi.org/10.1016/j.jtbi.2009.03.007>.
- Petit G, Anfodillo T, Carraro V, Grani F, Carrer M. 2011. Hydraulic constraints limit height growth in trees at high altitude. *New Phytol*. 189(1):241–252. <https://doi.org/10.1111/j.1469-8137.2010.03455.x>.
- Petit G, Anfodillo T, Mencuccini M. 2008. Tapering of xylem conduits and hydraulic limitations in sycamore (*Acer pseudoplatanus*) trees. *New Phytol*. 177(3):653–664. <https://doi.org/10.1111/j.1469-8137.2007.02291.x>.
- Petit G, Pfautsch S, Anfodillo T, Adams MA. 2010. The challenge of tree height in *Eucalyptus regnans*: when xylem tapering overcomes hydraulic resistance. *New Phytol*. 187(4):1146–1153. <https://doi.org/10.1111/j.1469-8137.2010.03304.x>.
- Petit G, Zambonini D, Hesse BD, Häberle KH. 2022. No xylem phenotypic plasticity in mature *Picea abies* and *Fagus sylvatica* trees after 5 years of throughfall precipitation exclusion. *Glob Chang Biol*. 28(15):4668–4683. <https://doi.org/10.1111/gcb.16232>.
- Petit G, Mencuccini M, Carrer M, Prendin AL, Hölttä T. 2023. Axial conduit widening, tree height and height growth rate set the hydraulic transition of sapwood into heartwood. *J Exp Bot*. 74(17): 5072–5087. <https://doi.org/10.1093/jxb/erad227>.
- Pfautsch S, Aspinwall MJ, Drake JE, Chacon-Doria L, Langelaan RJA, Tissue DT, Tjoelker MG, Lens F. 2018. Traits and trade-offs in whole-tree hydraulic architecture along the vertical axis of *Eucalyptus grandis*. *Ann Bot*. 121(1):129–141. <https://doi.org/10.1093/aob/mcx137>.
- Prendin AL, Petit G, Fonti P, Rixen C, Dawes MA, von Arx G. 2018. Axial xylem architecture of *Larix decidua* exposed to CO₂ enrichment and soil warming at the tree line. *Funct Ecol*. 32(2): 273–287. <https://doi.org/10.1111/1365-2435.12986>.
- R Core Team. 2021. R: A language and environment for statistical computing. R Foundation for Statistical Computing, Vienna, Austria.
- Ray DM, Jones CS. 2018. Scaling relationships and vessel packing in petioles. *Am J Bot*. 105(4):667–676. <https://doi.org/10.1002/ajb2.1054>.
- Rita A, Pericolo O, Saracino A, Borghetti M. 2020. Sperry’s packing rule affects the spatial proximity but not clustering of xylem conduits: the case of *Fagus sylvatica* L. *IAWA J*. 42(2):191–203.
- Rodriguez-Zaccaro FD, Daniela Rodriguez-Zaccaro F, Valdovinos-Ayala J, Percolla MI, Venturas MD, Pratt RB, Jacobsen AL. 2019. Wood structure and function change with maturity: age of the vascular cambium is associated with xylem changes in current-year growth. *Plant Cell Environ*. 42(6):1816–1831. <https://doi.org/10.1111/pce.13528>.
- Rosell JA, Olson ME, Anfodillo T. 2017. Scaling of xylem vessel diameter with plant size: causes, predictions and outstanding questions. *Curr For Rep*. 3(1):46–59. <https://doi.org/10.1007/s40725-017-0049-0>.
- Savage VM, Bentley LP, Enquist BJ, Sperry JS, Smith DD, Reich PB, Von Allmen EI. 2010. Hydraulic trade-offs and space filling enable better predictions of vascular structure and function in plants. *Proc Natl Acad Sci USA*. 107(52):22722–22727. <https://doi.org/10.1073/pnas.1012194108>.
- Schreiber SG, Hacke UG, Hamann A. 2015. Variation of xylem vessel diameters across a climate gradient: insight from a reciprocal transplant experiment with a widespread boreal tree. *Funct Ecol*. 29(11): 1392–1401. <https://doi.org/10.1111/1365-2435.12455>.
- Shaw M, Rights JD, Sterba SS, Flake JK. 2023. r2mlm: an R package calculating R-squared measures for multilevel models.

- Behav Res Methods. 55(4):1942–1964. <https://doi.org/10.3758/s13428-022-01841-4>.
- Shinozaki K, Yoda K, Hozumi K, Kira T. 1964a. A quantitative analysis of plant form—the pipe model theory I. Basic analyses. *Jpn J Ecol.* 14(3):94–105.
- Shinozaki K, Yoda K, Hozumi K, Kira T. 1964b. A quantitative analysis of plant form—the pipe model theory: II. Further evidence of the theory and its application in forest ecology. *Jpn J Ecol.* 14(4): 133–139.
- Sopp SBD, Valbuena R. 2023. Vascular optimality dictates plant morphology away from Leonardo's rule. *Proc Natl Acad Sci USA.* 120(39):e2215047120. <https://doi.org/10.1073/pnas.2215047120>.
- Stoffel MA, Nakagawa S, Schielzeth H. 2017. rptR: repeatability estimation and variance decomposition by generalized linear mixed-effects models. *Methods Ecol Evol.* 8(11):1639–1644. <https://doi.org/10.1111/2041-210X.12797>.
- Stoffel MA, Nakagawa S, Schielzeth H. 2021. partR2: partitioning R2 in generalized linear mixed models. *PeerJ.* 9:e11414. <https://doi.org/10.7717/peerj.11414>.
- Tokumoto I, Heilman JL, Schwinning S, McInnes KJ, Litvak ME, Morgan CLS, Kamps RH. 2014. Small-scale variability in water storage and plant available water in shallow, rocky soils. *Plant Soil.* 385(1–2):193–204. <https://doi.org/10.1007/s11104-014-2224-4>.
- Tyree MT, Ewers FW. 1991. The hydraulic architecture of trees and other woody plants. *New Phytol.* 119(3):345–360.
- Tyree MT, Zimmermann MH. 2002. Xylem structure and the ascent of sap. Springer, Berlin, Germany.
- Warton DI, Duursma RA, Falster DS, Taskinen S. 2012. 'Smatr 3'—an R package for estimation and inference about allometric lines. *Methods Ecol Evol.* 3(2):257–259. <https://doi.org/10.1111/j.2041-210X.2011.00153.x>.
- Weithmann G, Palgi SS, Schuldt B, Leuschner C. 2022. Branch xylem vascular adjustments in European beech in response to decreasing water availability across a precipitation gradient. *Tree Physiol.* 42(11):2224–2238. <https://doi.org/10.1093/treephys/tpac080>.
- Weitz JS, Ogle K, Horn HS. 2006. Ontogenetically stable hydraulic design in woody plants. *Funct Ecol.* 20(2):191–199. <https://doi.org/10.1111/j.1365-2435.2006.01083.x>.
- West GB, Brown JH, Enquist BJ. 1997. A general model for the origin of allometric scaling laws in biology. *Science.* 276(5309):122–126. <https://doi.org/10.1126/science.276.5309.122>.
- West GB, Brown JH, Enquist BJ. 1999. A general model for the structure and allometry of plant vascular systems. *Nature.* 400(6745): 664–667. <https://doi.org/10.1038/23251>.
- Williams CB, Anfodillo T, Crivellaro A, Lazzarin M, Dawson TE, Koch GW. 2019. Axial variation of xylem conduits in the Earth's tallest trees. *Trees.* 33(5):1299–1311. <https://doi.org/10.1007/s00468-019-01859-w>.
- Woodruff DR, Meinzer FC. 2011. In: Meinzer FC, Lachenbruch B, Dawson TE (eds), Size-dependent changes in biophysical control of tree growth: the role of turgor, in size- and age-related changes in tree structure and function. Springer: Netherlands, Dordrecht, pp. 363–384.
- Yang D, Zhang Y, Zhou D, Zhang YJ, Peng G, Tyree MT. 2021. The hydraulic architecture of an arborescent monocot: ontogeny-related adjustments in vessel size and leaf area compensate for increased resistance. *New Phytol.* 231(1):273–284. <https://doi.org/10.1111/nph.17294>.
- Zanne AE, Westoby M, Falster DS, Ackerly DD, Loarie SR, Arnold SEJ, Coomes DA. 2010. Angiosperm wood structure: global patterns in vessel anatomy and their relation to wood density and potential conductivity. *Am J Bot.* 97(2):207–215. <https://doi.org/10.3732/ajb.0900178>.
- Zhong M, Castro-Díez P, Puyravaud J-P, Sterck FJ, Cornelissen JHC. 2019. Convergent xylem widening among organs across diverse woody seedlings. *New Phytol.* 222(4):1873–1882. <https://doi.org/10.1111/nph.15734>.
- Zuur AF, Ieno EN, Walker NJ, Saveliev AA, Smith GM. 2009. Mixed effects models and extensions in ecology with R, Vol. 574. Springer, New York, p 574.